Proposing a new iterative learning control algorithm based on a non-linear least square formulation - Minimising draw-in errors

Endelt, B.

Published in:
Journal of Physics: Conference Series

DOI (link to publication from Publisher):
10.1088/1742-6596/896/1/012036

Publication date:
2017

Document Version
Publisher's PDF, also known as Version of record

Proposing a new iterative learning control algorithm based on a non-linear least square formulation - Minimising draw-in errors

IOP Conf. Series: Journal of Physics: Conf. Series **896** (2017) 012036 doi:10.1088/1742-6596/896/1/012036

Proposing a new iterative learning control algorithm based on a non-linear least square formulation - Minimising draw-in errors.

B. Endelt

Department of Materials and Production, Faculty of engineering and science, Aalborg University, Denmark

E-mail: endelt@make.aau.dk

Abstract. Forming operation are subject to external disturbances and changing operating conditions e.g. new material batch, increasing tool temperature due to plastic work, material properties and lubrication is sensitive to tool temperature. It is generally accepted that forming operations are not stable over time and it is not uncommon to adjust the process parameters during the first half hour production, indicating that process instability is gradually developing over time. Thus, in-process feedback control scheme might not-be necessary to stabilize the process and an alternative approach is to apply an iterative learning algorithm, which can learn from previously produced parts i.e. a self learning system which gradually reduces error based on historical process information. What is proposed in the paper is a simple algorithm which can be applied to a wide range of sheet-metal forming processes. The input to the algorithm is the final flange edge geometry and the basic idea is to reduce the least-square error between the current flange geometry and a reference geometry using a non-linear least square algorithm. The ILC scheme is applied to a square deep-drawing and the Numisheet'08 S-rail benchmark problem, the numerical tests shows that the proposed control scheme is able control and stabilise both processes.

1. Introduction

It is generally accepted that deep drawing and stamping operations are non-static over time i.e. changes in the material parameters, friction and lubrication, tool and press deflection, etc. all influence the process stability [1, 2].

A significant numbers of process control system has been proposed in the literature, classical PID regulators, meta models, expert systems, databases, optimal control, iterative learning control, Allwood *et al* gives a comprehensive review, covering the last two decades development within the field [3]. Endelt and Volk [4] identified two major obstacles which needs to be addressed before an industrial implementation is possible:

- The proposed control algorithms are often limited by the ability to sample process data with both sufficient accuracy and robustness - this lack of robust sampling technologies is one of the main barriers preventing successful industrial implementation.
- Limitation in the current press designs; many of the presses currently used in industry only offer limited opportunities to change the blank-holder force during the punch stroke. Even if, the press offers the opportunity to change the blank-holder force the reaction speed may be insufficient compared with the production rate in an industrial application.

Endelt and Volk proposed an alternative control system, where the process parameters were updated based on historical process data, the algorithm were tested numerically and the control system successfully stabilised the process. However, the control system were design for a square deep-drawing process and the approach can not be directly adopted to a new tool geometry. This problem is addressed in the present work, where a general algorithm is proposed, enabling process control of stamping and deep-drawing processes, using post process sampling of the flange geometry. The proposed algorithm was tested numerically using both a square cup and the Numisheet'08 S-rail benchmark problem.

2. Iterative learning control Algorithm

The iterative learning algorithm is based on the Non-linear least square methods were the flange fitting problem is solved through the definition of an objective function $f(\boldsymbol{x})$:

$$f(\boldsymbol{x}_k) = \frac{1}{2}\boldsymbol{r}_k^T \boldsymbol{r}_k \tag{1}$$

Where $\boldsymbol{x}_k$ and $\boldsymbol{r}(\boldsymbol{x}_k)$ represent the adjustable process parameters and the residual vector, respectively. The residual vector represents the error between the current flange geometry $\boldsymbol{y}_k$ and an reference flange geometry $\boldsymbol{y}^{ref}$

$$\boldsymbol{r}_k = \boldsymbol{y}_k - \boldsymbol{y}^{ref}$$

where k is the iteration counter.

The objective function is approximated by a quadratic function defined as:

$$f(\boldsymbol{x}_k + \boldsymbol{s}_k) = f(\boldsymbol{x}_k) + \nabla f(\boldsymbol{x}_k)^T \boldsymbol{s}_k + \frac{1}{2}\boldsymbol{s}_k \boldsymbol{H} \boldsymbol{s}_k^T \tag{2}$$

$$\nabla f(\boldsymbol{x}_k) = \boldsymbol{J}(\boldsymbol{x}_k)^T \boldsymbol{r}(\boldsymbol{x}_k) \tag{3}$$

$$\boldsymbol{H} \approx \boldsymbol{J}(\boldsymbol{x}_k)^T \boldsymbol{J}(\boldsymbol{x}_k) \tag{4}$$

Where $\nabla f(\boldsymbol{x}_k)$ and $\boldsymbol{H}$ represent the gradient and the Hessian respectively, a Gauss-Newton formulation is used to approximate the Hessian matrix using only first order information from the Jacobian matrix $\boldsymbol{J}(\boldsymbol{x}_k)$.

If the minimization problem is assumed to be positive definite the step s_k can be calculated as:

$$\boldsymbol{s}_k = -\alpha \frac{\nabla f(\boldsymbol{x})}{\boldsymbol{H}} \text{ and } \boldsymbol{x}_{k+1} = \boldsymbol{x}_k + \boldsymbol{s}_k$$

This is known as a line search problem where α is a scalar parameter controlling the step size i.e. scaling the change in the process parameters $\boldsymbol{x}$, for the current application a fixed a value is applied.

2.1. Iterative learning scheme

The above algorithm is a classical formulation of a non-linear curve fitting problem, where the Jacobian matrix is calculated for each iteration k, using either an analytical representation or a finite difference approximation.

The non-linear optimization algorithm, can be reformulated to an iterative learning control scheme. If the flange fitting problem is assumed to be convex and close to linear, in a sufficient region surrounding the optimal process parameters $\boldsymbol{x}^*$ which also defines the optimal flange geometry. Under these assumptions, it is only necessary to calculate the Jacobian representation at the point $\boldsymbol{x}^*$. Thus, only one Jacobian matrix is defined $\boldsymbol{J}(\boldsymbol{x}^*)$, which will govern the optimization problem, for any set of parameters $\boldsymbol{x}_k$ and any residual vector $\boldsymbol{r}_k$ which are sufficient

close to $\boldsymbol{x}^*$. The Jacobian is a $m \times n$ matrix, where n represents in this case represents the number of process parameters $\boldsymbol{x}$ and m represents the number of sample points $\boldsymbol{y}$. The j-th column of the Jacobian matrix gives the sensitivity of the flange draw-in error $\boldsymbol{r}$ with respect to the process parameter x_j. The vectors $\partial \boldsymbol{r}/\partial x_j$ represents the sensitivity of each sample point i with respect to process parameters x_j.

1: Choose the "optimal" process parameters x^* and the step size scalar α and s_{max}, load or sample the reference flange geometry $\boldsymbol{y}^{ref}$. Initialize the counter $k = 1$, k_{max} and set $\boldsymbol{x}_k = \boldsymbol{x}^*$.
2: Load the Jacobian matrix $\boldsymbol{J}(\boldsymbol{x}^*)$ and calculate the Hessian matrix using the Gauss-Newton approximation $\boldsymbol{H}^* \approx \boldsymbol{J}(\boldsymbol{x}^*)^T \boldsymbol{J}(\boldsymbol{x}^*)$
3: **while** $(k < k_{max})$ **do**
4: Update the flange geometry $\boldsymbol{y}_k$, the residual vector and the gradient according to:
5: Residual vector: $\boldsymbol{r}_k = \boldsymbol{y}_k - \boldsymbol{y}^{ref}$
6: Gradient: $\nabla f(\boldsymbol{x}_k) = \boldsymbol{J}(\boldsymbol{x}^*)^T \boldsymbol{r}(\boldsymbol{x}_k)$
7: $\boldsymbol{d}_k = -\frac{\nabla f(\boldsymbol{x}_k)}{\boldsymbol{H}^*}$
8: Calculating maximum step size according to:
9: **if** $(s_{max} > 0)$ **then**
10: $\alpha_{max} = \min\left(\alpha, \frac{s_{max}}{\max(\max(\boldsymbol{d}_k), -\min(\boldsymbol{d}_k))}\right)$
11: **else**
12: $\alpha_{max} = \alpha$
13: **end if**
14: Update the process parameters $\boldsymbol{x}_{k+1}$ according to:
$\boldsymbol{x}_{k+1} = \boldsymbol{x}_k - \alpha_{max} \frac{\nabla f(\boldsymbol{x}_k)}{\boldsymbol{H}^*}$
15: $k = k + 1$
16: **end while**
17: End

Fig. 1: Flange fitting iterative learning control algorithm based on a non-linear least square formulation. The Jacobian matrix is approximated using finite difference and it is only calculated for the reference point $\boldsymbol{x}^*$.

3. Numerical models

The stability and performance of proposed ILC algorithm are tested numerically. Furthermore, diversity of the application areas are tested applying the ILC algorithm on two very different sheet metal forming processes:

- A square deep-drawing enabling full control of the flange draw-in using a special designed shimming system, where the blank-holder is locally deformed using hydraulic pressure. The deflection of the blank-holder is controlled by four cavities located on each side of the square cup, giving a total of five process parameters, including the blank-holder force, which can be individual adjusted, see figure 2(a). 32 sample points were collected along the flange edge, see figure 2(b).
- The S-rail Benchmark 2 from Numisheet 2008 were used as a second example and the model were developed according to the benchmark description [5]. Additionally, the die is supported by 10 individual controlled hydraulic punches (hydraulic cushion system), evenly distributed along each side of the S-rail, positioned just before the sheet metal enters the draw beads, see figure 3(a). 23 points were sampled from each flange edge (a total of 46 sample points), see figure 3(b)

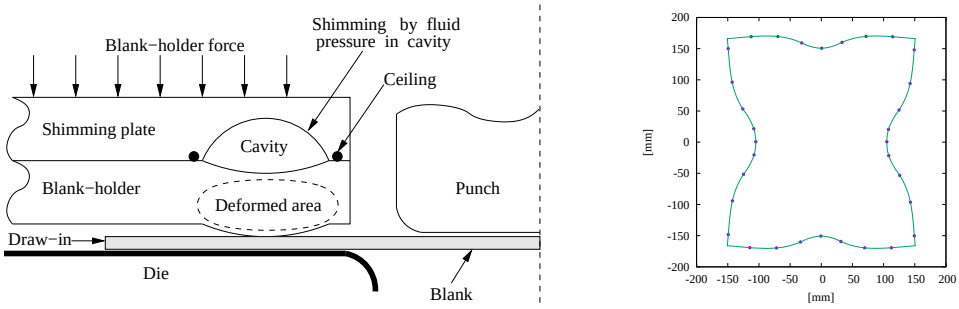

(a) Illustration of the shimming scheme [6].

(b) Reference edge - represented by 32 samples.

Fig. 2: Square deep-drawing input and reference flange geometry.

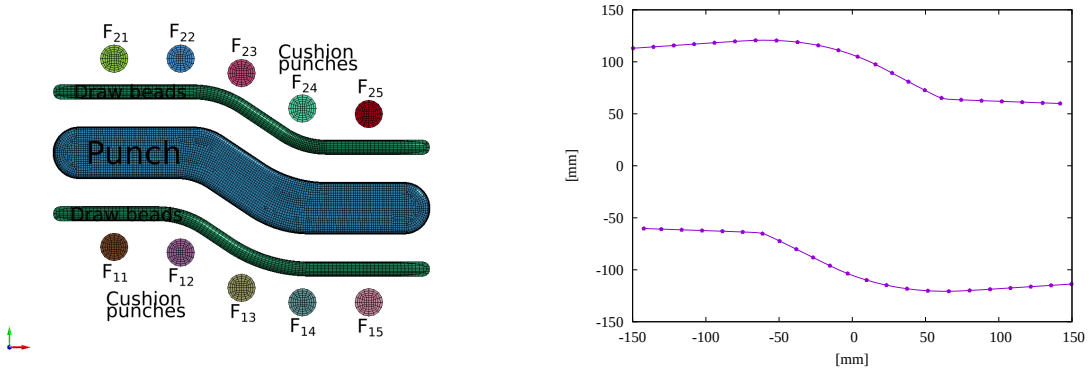

(a) Naming convention and location of the cushion punches.

(b) Reference edge - 23 sample points on each side.

Fig. 3: S-rail input and reference flange geometry.

4. ILC configuration

The main component in the proposed ILC algorithm is the Jacobian matrix $\boldsymbol{J}(\boldsymbol{x}^*)$ and step size scaling parameter α. The framework was developed using the finite element code LS-Dyna and a successful ILC algorithm should be able to

- In the case where only process parameters has been manipulated - the system should return to the reference parameters $\boldsymbol{x}^*$.
- The system should only react on repetitive errors (new material batch, increased tool temperature etc.), thus the system should be conservative with respect changing process parameters (controlled by α).
- $J(\boldsymbol{x}^*)$ is only calculated for the reference x* and to avoid shooting process parameters due to inaccurate between the process model and the current state of the process, a limiting step size regulation were implemented, see figure 1.

4.1. Square deep drawing

Reference process parameters $\boldsymbol{x}^*$, disturbances and perturbations used for the forward difference approximation of the Jacobian matrix are listed in table 1.

Table 1: Cavity pressure and blank-holder force applied during system evaluation, see figure 2(a). The Jacobian matrix is estimated using forward difference approximation using the perturbation $\Delta \boldsymbol{x}$.

	P_1	P_2	P_3	P_4	F_{BH}
Reference $\boldsymbol{x}^*$	15MPa	15MPa	15MPa	15MPa	250kN
Disturbance	5MPa	25MPa	5MPa	25MPa	350kN
Perturbation $\Delta \boldsymbol{x}$	0.015MPa	0.015MPa	0.015MPa	0.015MPa	0.250kN

There was a clear correlation between the step size α and the system response. Furthermore, unstable behaviour can be provoked for $\alpha \geq 0.75$, see figure 4, the instability is due to non-linearities i.e. large deviation between the true $\boldsymbol{J}(\boldsymbol{x}_0)$ and $\boldsymbol{J}(\boldsymbol{x}^*)$ the algorithm can be stabilised using $\alpha \leq 0.5$ or constraining the maximum step size s_{max}, see line 9-13 figure 1. Based on the system responses figure 4 $\alpha = 0.5$ and $s_{max} = 100kN$ (maximum allowed change in F_{bh} in one iteration) represent a reasonable trade-off between the controller response and system damping.

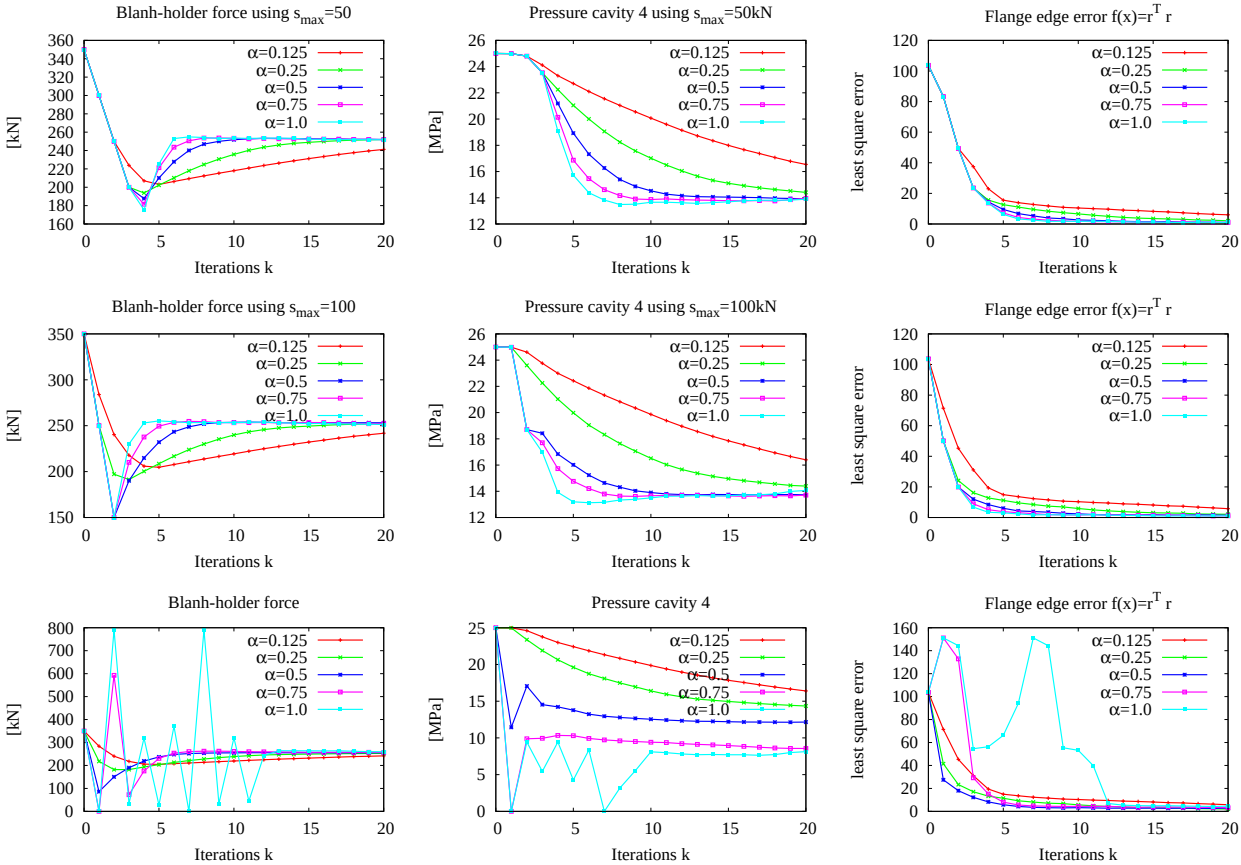

Fig. 4: Square deep-drawing system response for various α values. Note, the overshot for high α values and the unstable system behaviour for $\alpha \geq 0.75$. Further, large changes in the input parameters can be avoided by constraining the maximum step size - in the case the blank-holder input is constrained ($s_{max} = 50$ and 100kN).

4.2. S-rail Numisheet'2008 benchmark
The reference cushion punch forces is listed in table 2 again the system is forces out of balance and the ability to retrieve the reference input values and the rate of convergence are tested for different α values, see figure 5.

Table 2: Cushion punch forces applied for the system evaluation (total blank-holder force is 820kN), see figure 3(a). The Jacobian matrix is estimated using forward difference approximation using the perturbation $\Delta \boldsymbol{x}$.

	F_{11} and F_{25}	F_{12} and F_{24}	F_{13} and F_{23}	F_{14} and F_{22}	F_{15} and F_{21}
Reference $\boldsymbol{x}^*$	110kN	60kN	80kN	60kN	100kN
Disturbance $F_{11} - F_{15}$	175kN	110kN	30kN	10kN	150kN
Disturbance $F_{21} - F_{25}$	35kN	10kN	30kN	10kN	150kN
Perturbation $\Delta \boldsymbol{x}$	2kN	2kN	2kN	2kN	2kN

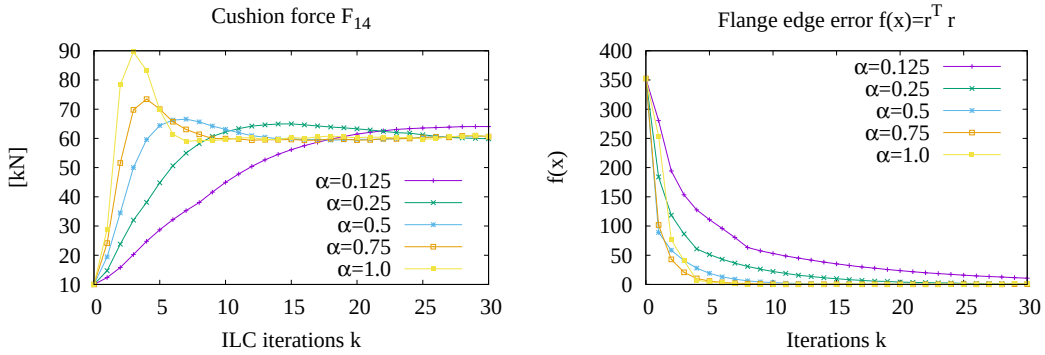

Fig. 5: System response for various α values. Note, the overshot for high α values.

There was a clear correlation between the step size scale factor α and the system response. The best performance is achieved using $\alpha = 0.5$ i.e. converges $\boldsymbol{x}^*$, limited overshoot and a relative fast reduction of the least square error, see figure 5.

5. Numerical performance test
The ILC system tested by substituting the reference material with a new material which has significant different material properties.

5.1. Square deep drawing using $\alpha = \frac{1}{2}$ and $s_{max} = 100kN$
For square deep-drawing a new blank material with an uneven thickness distribution mm (0.95 to 1.05mm left to right) and changes in the material parameters, see figure 9.

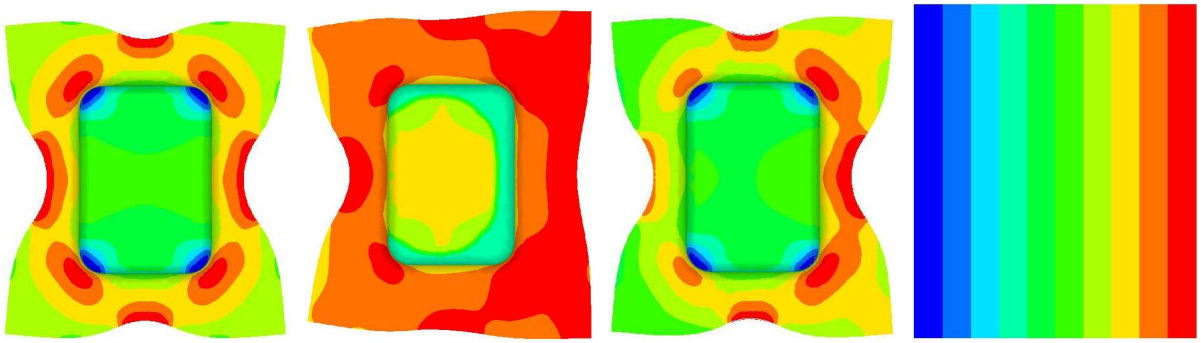

(a) Reference part (material parameters: K=550MPa and n=0.25) thickness range 0.68-1.16mm

(b) ILC part first iteration. Thickness range 0.26-1.21mm

(c) ILC part after 20 iteration. Thickness range 0.67-1.19mm.

(d) ILC blank, initial thickness range 0.95-1.05mm, Material parameters K=450 and n=0.23

Fig. 6: The proposed ILC algorithm has a remarkable influence on the process stability. Not only is the error flange draw-in error minimised but also the severe thinning observed in the first iteration (b) is gradually eliminated by the ILC scheme (c).

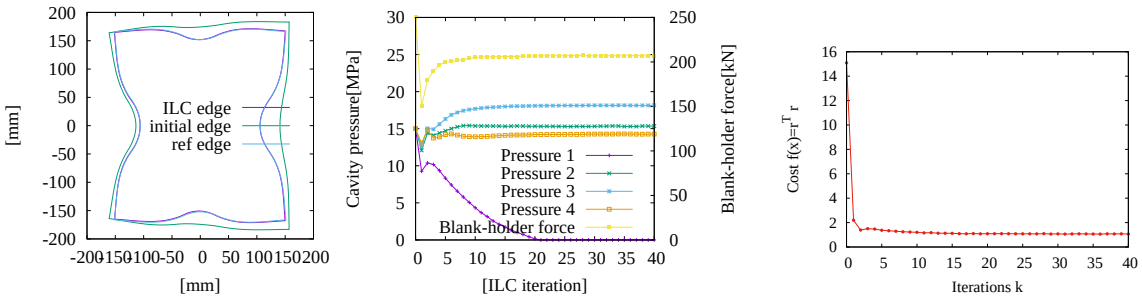

(a) Flange edge.

(b) Process parameters as a function of ILC iteration.

(c) Least square flange draw-in error

Fig. 7: Process variables as a function of ILC iterations

5.2. S-rail using $\alpha = \frac{1}{2}$ *and* $s_{max} = 100kN$

The reference flange geometry for the S-rail was produced using material 1 (HC260LAD) and a new material is introduced using material 2 (Al170), see table 3.

Table 3: Ghosh hardening parameters for the two materials specified in the S-rail Numisheet'08 benchmark.

	A	ϵ_0	C	n	R_{00}	R_{45}	R_{90}
Material 1 (HC260LAD)	1068.8	0.009	433.1	0.097	1.12	0.86	1.5
Material 2 (Ac-170)	872.8	0.017	479.8	0.1	0.67	0.45	0.62

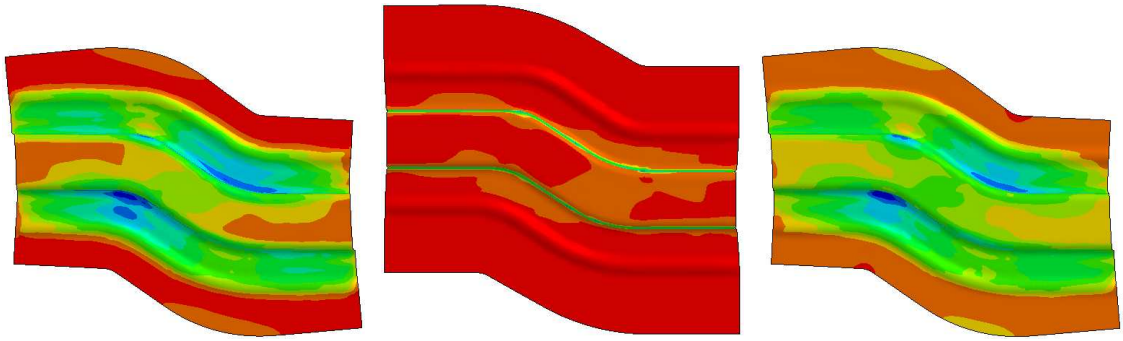

(a) Reference part using material 1 HC260LAD thickness range 0.82-1.01mm

(b) ILC part first iteration using material 2 Ac-170 material parameters. Thickness range 0.07-1.0mm

(c) ILC part after 20 iteration using material 2 Ac-170. Thickness range 0.78-1.04mm.

Fig. 8: Not only is the error flange draw-in error minimised but also the severe thinning observed in the first iteration (b) is gradually eliminated by the ILC scheme (c).

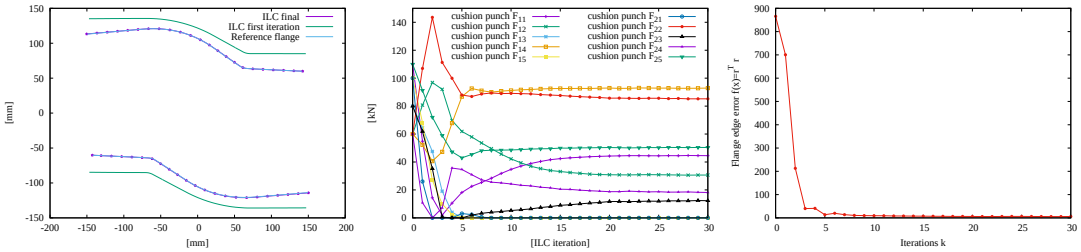

Fig. 9: The ILC algorithm converge to a stable process configuration, using 10 to 15 iteration, flowing the material change. The total cushion force converge to 335kN.

6. Conclusion

The proposed ILC algorithm proved very efficient for both the square deep-drawing and S-rail benchmark. In both cases the process instability was eliminated after only 5-10 iteration following the change of material properties. Furthermore, there are currently no indication that the system will encounter long term instability. However, further numerical tests and eventual experimental testing is need, to evaluate the long term performance of the system. The system only relay on post process data, thus data can be sampled after the tool is opened using, e.g. laser scanners, image processing. Furthermore, the sampling rate is independent of the production rate i.e. if the process is running stable the sample rate can be decreased and if the process is drifting or a new material batch are introduced the sample rate can be increased.

7. References

[1] Hora P, Heingartner J, Manopulo N and Tong L 2011 *NUMISHEET 2011* (American Institute of Physics)
[2] Roll K 2008 *Numisheet 2008* pp 3–11
[3] Allwood J, Duncan S, Cao J, Groche P, Hirt G, Kinsey B, Kuboki T, Liewald M, Sterzing A and Tekkaya A 2016 *CIRP Annals-Manufacturing Technology* **65** 573–596
[4] Endelt B and Volk W 2013 *Proceedings of the IDDRG 2013 Conference, Best in Class Stamping* submitted for presentation at the IDDRG 2013 Conference
[5] 2008 *Numisheet Benchmark 2008* (ETH Zurich, Institute of Virtual Manufacturing) chap Influence of Draw Beads on the Springback Behavior
[6] Endelt B, Tommerup S and Danckert J 2013 *Journal of Materials Processing Technology* **213** 36 – 50 ISSN 0924-0136